Design for a Gravitational Wave Generator/Thruster V8
Part I

Peter CM Hahn
September 1, 2025

Abstract

This device generates gravitational waves which can be utilized as a thruster or as a communication device. It is comprised of a linear antenna array that is injected with a Radio Frequency (RF) signal. The antennas are configured to convert electromagnetic (EM) waves into gravitational waves.

When the antennas are arranged in a linear phased-array configuration, a thrust is produced that allows the device to be used as a method of propulsion. Part I of this article describes the device when configured as a thruster and documents the test results.

Part II will document the test results of the device when configured as a gravitational wave transmitter. If the injected RF signal is modulated with an Intermediate Frequency (IF) signal, the gravitational waves produced are also modulated. The invention can then function as a communication device by using the gravitational waves as a carrier instead of EM waves. A gravitational wave detector at the receiving end can demodulate the gravitational waves, thereby extracting the original (IF) signal.

Table of Contents

List of Figures

List of Photos

List of Tables

Background Theory

Foamy Ether Theory (FET) [1] describes electromagnetic (EM) waves as distortions in the foam that are transverse to the direction of propagation. Figure 1a below shows that the foamy ether has maximum distortion (compression) at the positive and negative peaks of the EM wave. A gravitational wave, however, is a compression that is parallel to the direction of propagation (see Figure 1b). This is explained in more detail at: https://www.peterhahn.ca/the-photon.

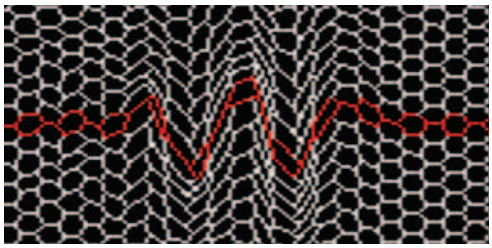

Figure 1a
EM wave through foamy ether

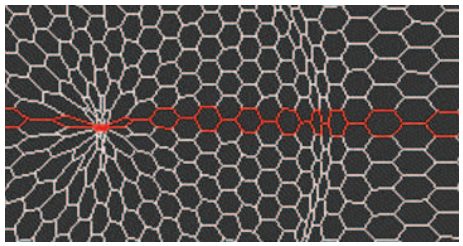

Figure 1b
Gravitational wave through foamy ether

According to FET, when two EM waves traveling in opposite directions meet, a compression of foamy ether (space) takes place between the waves. Screen captures of a simulation (using *ThreeDimSim*) of this compression is illustrated in Figures 2a to 2f. The figures show how the foamy ether is distorted by an array of four antenna pairs that are fed phase-shifted EM waves. The top red bar is a cross section of an antenna element where the RF signal is flowing towards the viewer, while the bottom red bar has the RF signal flowing away from the viewer. Figure 2a shows the beginning of the distortion

created by the first antenna pair, followed by Figures 2b to 2d which show the progression. Figures 2e to 2f show how the compression wave continues to travel to the right even after the EM waves have completed their vertical distortions. This compression wave is equivalent to a gravitational wave. (Notice that no compression wave leaves the left side of the antenna array).

The full simulation can be viewed at: https://www.peterhahn.ca/gravitational-wave-generator.

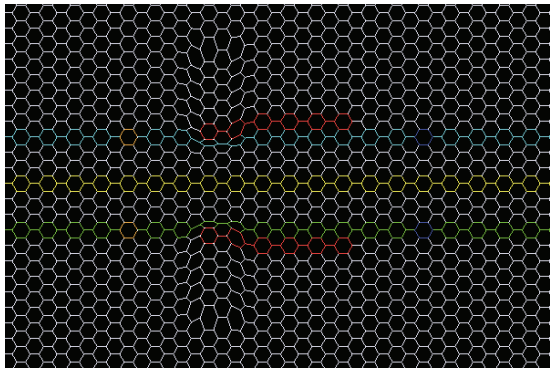

Figure 2a
EM Pulse on Antenna #1

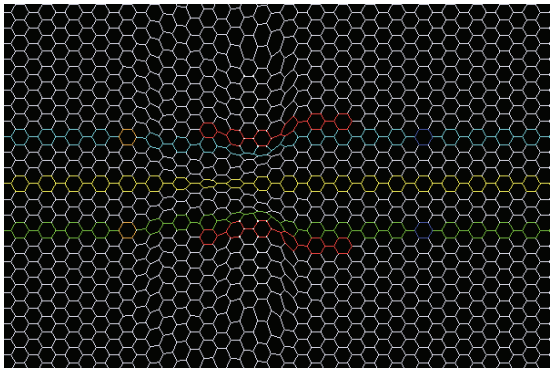

Figure 2b
EM Pulse on Antenna #2

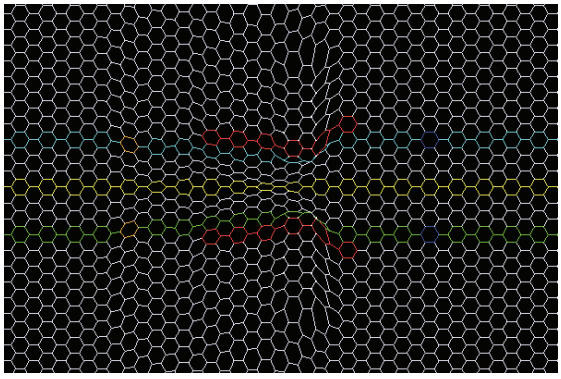

Figure 2c
EM Pulse on Antenna #3

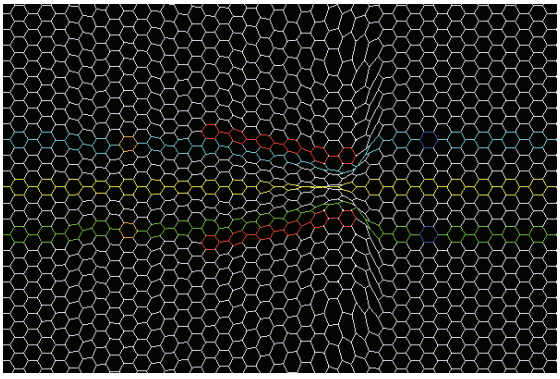

Figure 2d
EM Pulse on Antenna #4

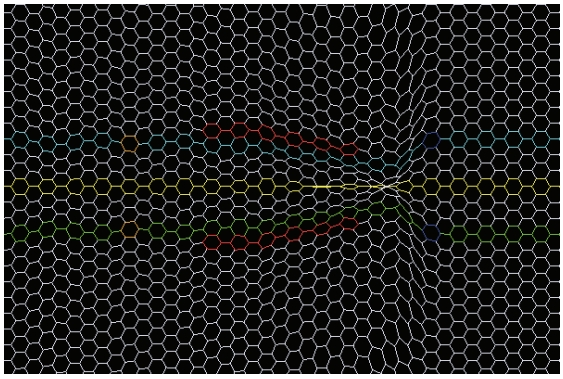

Figure 2e
Gravitational wave exits antenna array

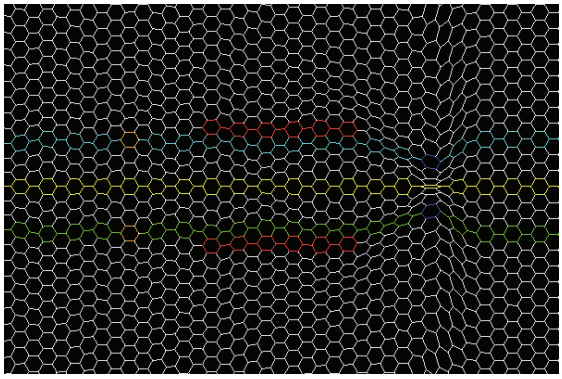

Figure 2f
Gravitational wave continues

The vertical distances between the orange cells on the left and the dark blue cells on the right were plotted in Figure 3a and 3b while the simulation was running. Figure 3a plots the vertical distances between the orange cells (orange line) and the dark blue cells (blue line) while the compression wave travels through the array. The sum of these *compressions* between the two dark blue cells on the right equals 339 (area between horizontal time points 9 and 29). The sum of the *stretching* for an equal amount of time (points 30 to 50) equals 113. Therefore, space on the right side of the array spends more time in a compressed state than in a stretched state. This imbalance will cause a force to occur on the device because the distortion pattern created between the blue cells is similar to the distortion created by the presence of matter. According to FET, the array will experience an attractive force towards this distortion.

Figure 3b shows an even greater imbalance when three pulses occur in succession. The first two pulses have a sum of compression values equaling 704, while the total time spent in a stretched state equals 57. Notice that much less distortion occurs on the left side of the simulation (orange line).

This process of using *phase-shifted, opposing* EM waves to create gravitational waves is the basis of this invention. Since the electric force is approximately 2.4×10^{43} times greater than the gravitational force [2], a significant thrust is therefore achieved.

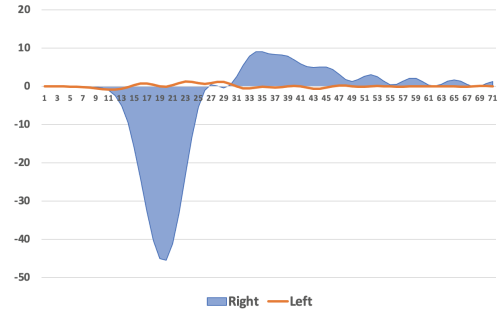

Figure 3a
Compression Plot: One Pulse

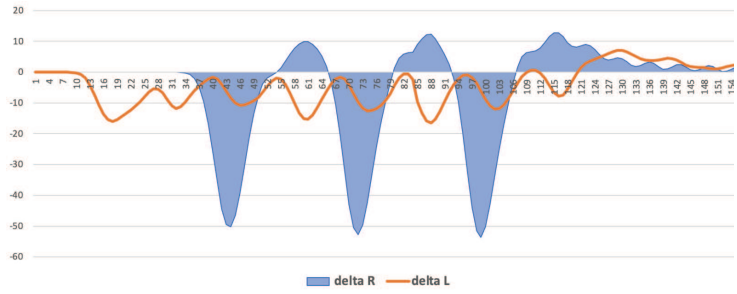

Figure 3b
Compression Plot: Three Pulses

(This vertical squeezing of space between two opposing EM waves is analogous to the process of squeezing out the last bit of toothpaste from a nearly empty tube. Using your thumb and forefinger, you start from the back and progressively squeeze the tube towards the opening, thereby expelling the toothpaste).

Applications of a GW Thruster

A gravitational wave thruster has the following advantages over current propulsion technologies:

- The EMDrive that claims to use high frequency microwaves as a source of thrust has been proven ineffective [3].
- This invention utilizes opposing electromagnetic waves to generate gravitational waves, thereby producing thrust without the need for propellant. As a result, spacecraft equipped with this technology could operate indefinitely, provided a

continuous electrical power source is available (e.g., solar energy). Potential applications as a propulsion system include maneuvering various objects such as:
    - Aircraft
    - Spacecraft (for lunar landings, asteroid mining operations, or planetary exploration)
    - Space-based telescopes (e.g., James Webb [4], Hubble [5])
    - Satellites
        - To maintain orbital altitude
        - For deorbiting during decommissioning
        - To navigate to legacy satellites for refueling purposes.
- Does not kick up dust while landing on the moon.
- The invention may also be used as a device that reduces the gravitational pull on an object when that object is placed between a GWT and the earth. The effect could potentially be strong enough to make the object essentially weightless, while still located on the surface of a planet. This could be used to run experiments in a weightless environment without the need for going into orbit.

Description of How the Device Works

An alternating current (i.e RF signal) that is fed through a conductor generates EM waves that propagate away from the conductor at the speed of light. However, if two conductors are placed adjacent to each other and fed an AC signal in opposing directions, there is a rhythmic compression and stretching of empty space between the conductors. This compression of space is similar to what occurs in a gravitational wave. The EM waves created by the two opposing signals cancel each other out, but the gravitational wave propagates into the surrounding space. The frequency of the gravitational wave is twice that of the frequency of the AC signal because a compression takes place each time the current flow changes direction and reaches a maximum.

The current prototype was built with the configuration illustrated in Figure 4. Oscillator (1) from Silicon Labs was used to generate a 466MHz continuous sinewave (however, any frequency will work). The output of the oscillator is connected to the input of a programable attenuator (2). This attenuator is used to set the power level and is also used as an on/off switch for the RF signal. The attenuator feeds a Low Noise Amplifier (3) which is connected to a six-way RF power divider (4). Five outputs of the power divider are connected to programmable attenuators (5) which feed into the phase shifters (6). These phase shifters provide adjustable phase shifts of the RF signal to each antenna array element (10). RF Power Amplifiers (7) provide a boost in the power level sent to each antenna element. The antenna array element (A) on the far left receives the RF signal first, followed by the next element to the right, until array element on the far right (E) receives the signal last. Each of the array elements are separated by 1/10th of a wavelength (≈6cm). A phase shift of 1/10th wavelength feeding the array elements, separated by 1/10th wavelength, creates a gravitational wave pulse that travels from left to right. The gravitational pulses exit the device on the right, thereby creating a thrust that *pulls* the device from left to right as indicated by arrow (11).

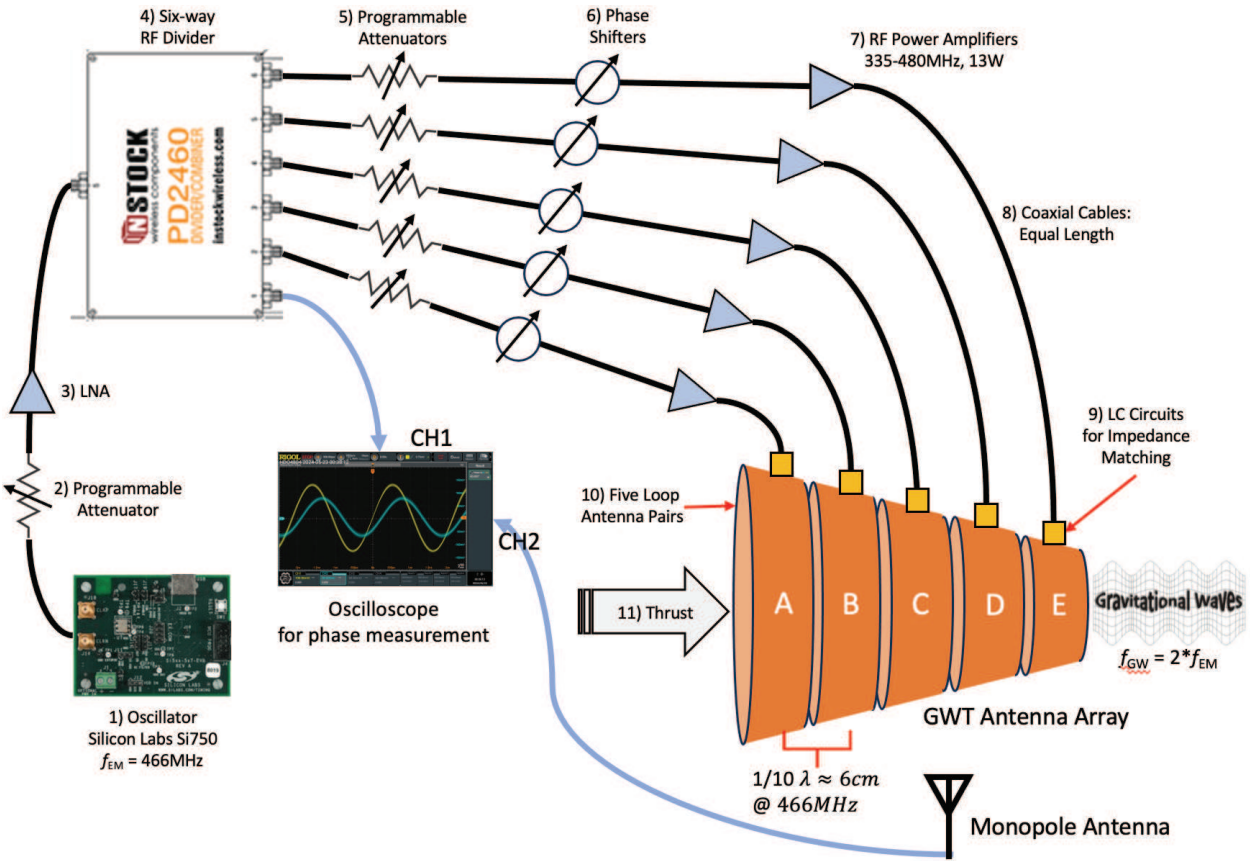

Figure 4
General Configuration of Prototype

The current prototype uses a pair of loop antennas that are placed adjacent to each other to form one antenna array element. Figure 5 shows a cutaway view of the internal components of one antenna array element. It is comprised of two concentric loop conductors insulated from each other. The two conductors are fed opposing AC currents that are 180 degrees out of phase. Loop antenna pair A (Figure 4) is constructed so its circumference is equal to one wavelength of the RF signal (64.3cm at 466MHz). Antenna elements B to E are constructed with progressively smaller diameters to provide further squeezing/compressing of space. An adjustable impedance matching LC circuit is attached to each antenna pair (see item 9 on Figure 4). (Theoretically, any antenna shape has the potential to generate gravitational waves, if it is configured, such that at least two insulated antennas are placed adjacent to each other and are fed opposing AC currents).

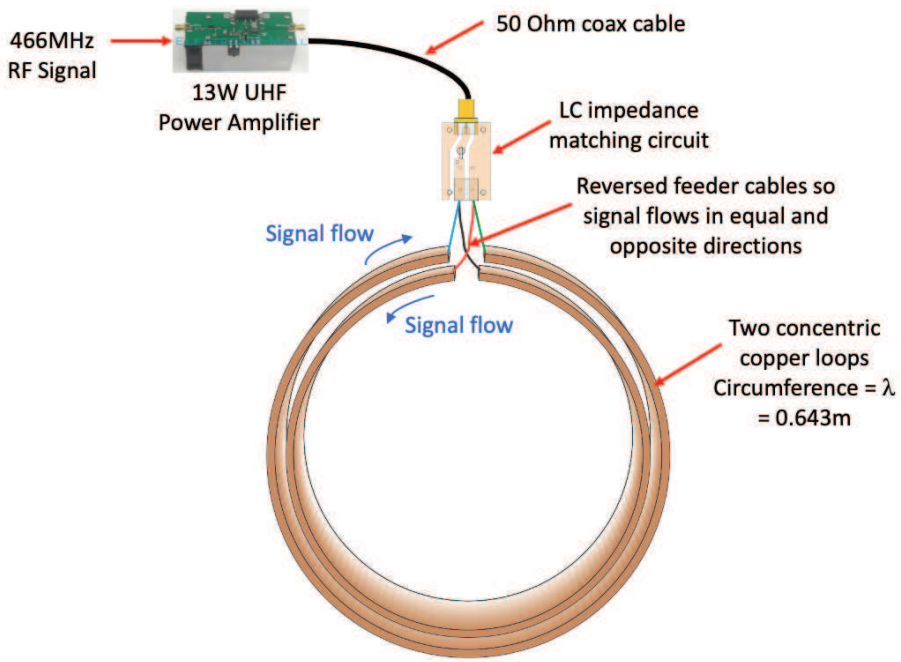

Figure 5
Cutaway of a Loop Antenna Element

Antenna Properties

A NanoVNA [4] (Vector Network Analyser) was used to measure the properties of the antenna array element prototypes. Plots of the results are as follows:

- Figure 6a is a Smith Chart [5] plotting the actual (unmatched) reactance values of the five antenna array elements. Resistance value is approximately 148Ω and reactance is -j177Ω at 466MHz.
- Figure 6b is the LC circuit needed to match the impedance of the antennas to a 50Ω coax cable.
- Figure 6c is a Smith Chart plot of the antenna elements with LC impedance matching circuits installed.
- Figure 6d is a plot of the Standing Wave Ratio (SWR) of matched antenna elements.

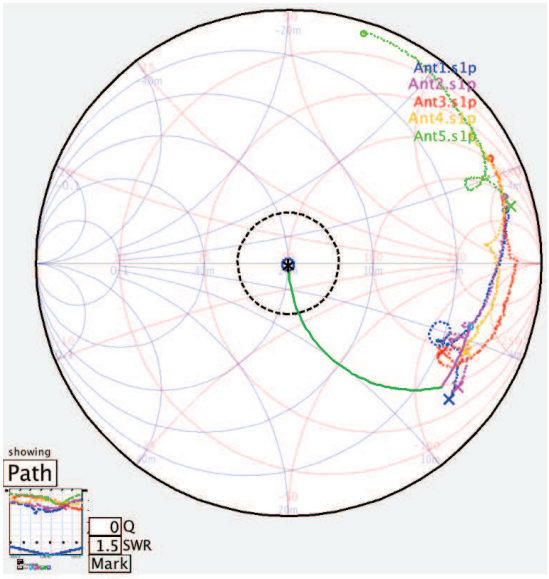

Figure 6a Smith Chart Plot
Unmatched Impedances

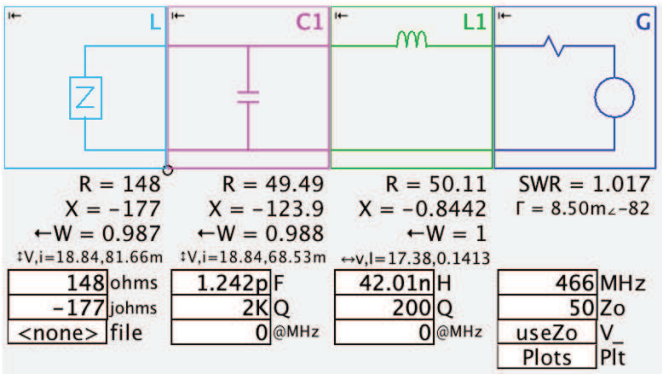

Figure 6b
Impedance Matching LC Circuit

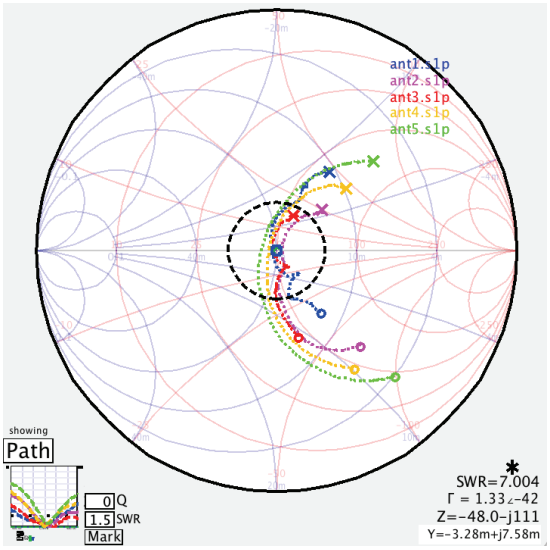

Figure 6c Smith Chart Plot
Matched Impedances
2025-07-07

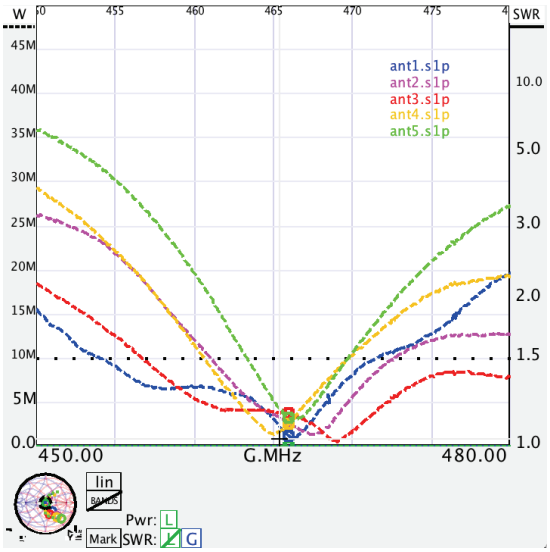

Figure 6d SWR Plot
Matched Impedances
2025-07-07

Phase Shift/Delay

Incremental phase delays between antenna elements are produced by using adjustable phase shifters (See Figure 4). Figure 7a is a calculated plot of five sinewaves where each wave is progressively shifted by 30 degrees. Figure 7b uses the same calculated values as Figure 7a but plots the *absolute value* of the sine waves instead. This is because a gravitational (compression) wave is produced at both the positive and negative portion of the RF sinewave. (The frequency of the resulting gravitational wave is twice that of the

RF signal). Figure 7b plots the amplitude and phase delay of each antenna element. (Best results were achieved when similar power levels were fed to each antenna element). Figure 7c is a polar plot that shows the phase delays and power levels of each antenna element.

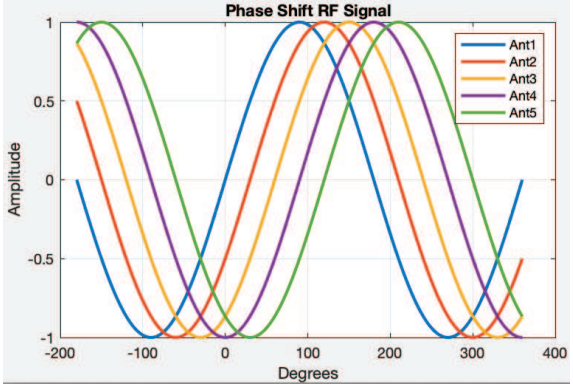

Figure 7a
Phase Delay 30^0 Calculated EM Waves
[0;30;60;90;120] Degrees

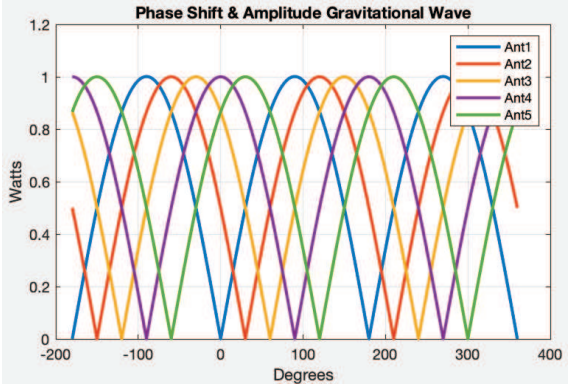

Figure 7b
Calculated Amplitude Plus Phase Delay
Gravitational Waves

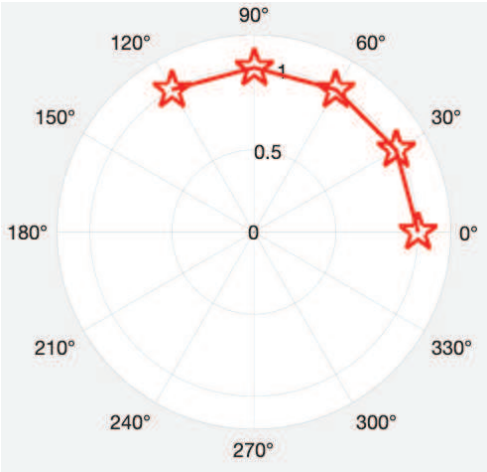

Figure 7c Polar Plot
Amplitude and Phase

V7 to V8 Enhancements

Version 8 (V8) incorporated the following enhancements to increase device sensitivity and reduce false positives.

1. The Styrofoam core was replaced with custom POM [6] plastic gaskets for securing the antenna elements to the array (see Photo 1). Unlike Styrofoam, POM material does not off-gas when placed in a vacuum, thereby preventing any potential generation of undesirable thrust.
2. The ends of the antenna array were covered to prevent airflow through the array.
3. RF amplifiers, phase shifters, and attenuators were shielded with copper to reduce crosstalk.

4. The aluminum support bracket was replaced with a nonconducting poster board.
5. Crossbeams and cross wires were added to the pendulum frame to limit movement to the x plane and reduce z plane movement (see Figure 9 and Photo 2).
6. The laser and webcam assemblies were detached from the test platform and installed on an adjacent wall 1.5 meters from the antenna array. This configuration was chosen to minimize magnetic attraction associated with their metal holders.

Measuring Thrust

Test Apparatus

Measuring the movement of the device was accomplished by using the test configuration as shown in Figures 8 and 9 and Photos 2 to 5. The antenna array was mounted on the base of a double pendulum device. The antenna array and mounting bracket assembly can be lifted out and rotated 180^{O} so that thrust can be measured in either direction. A laser diode projected the laser light onto a mirror which was fixed on the pendulum base at a 45^{O} angle. The laser beam reflected off the pendulum mirror and the stationary mirror which was picked up by a webcam (lens removed). The output of the webcam was fed into a computer which recorded the left and right movement of the device.

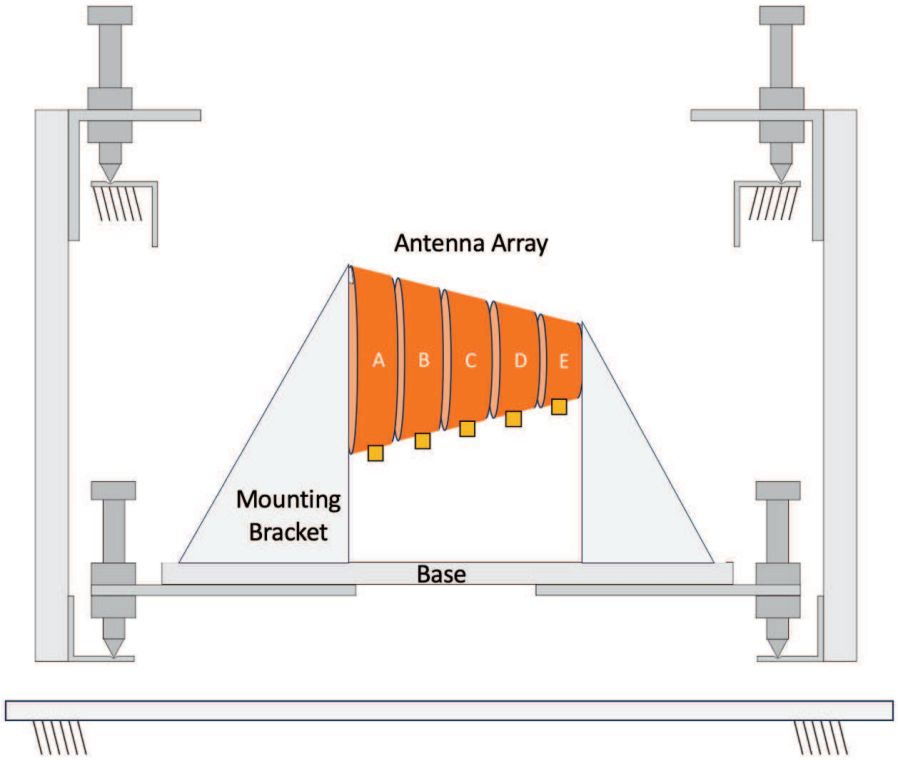

Figure 8
Pendulum and Antenna Array

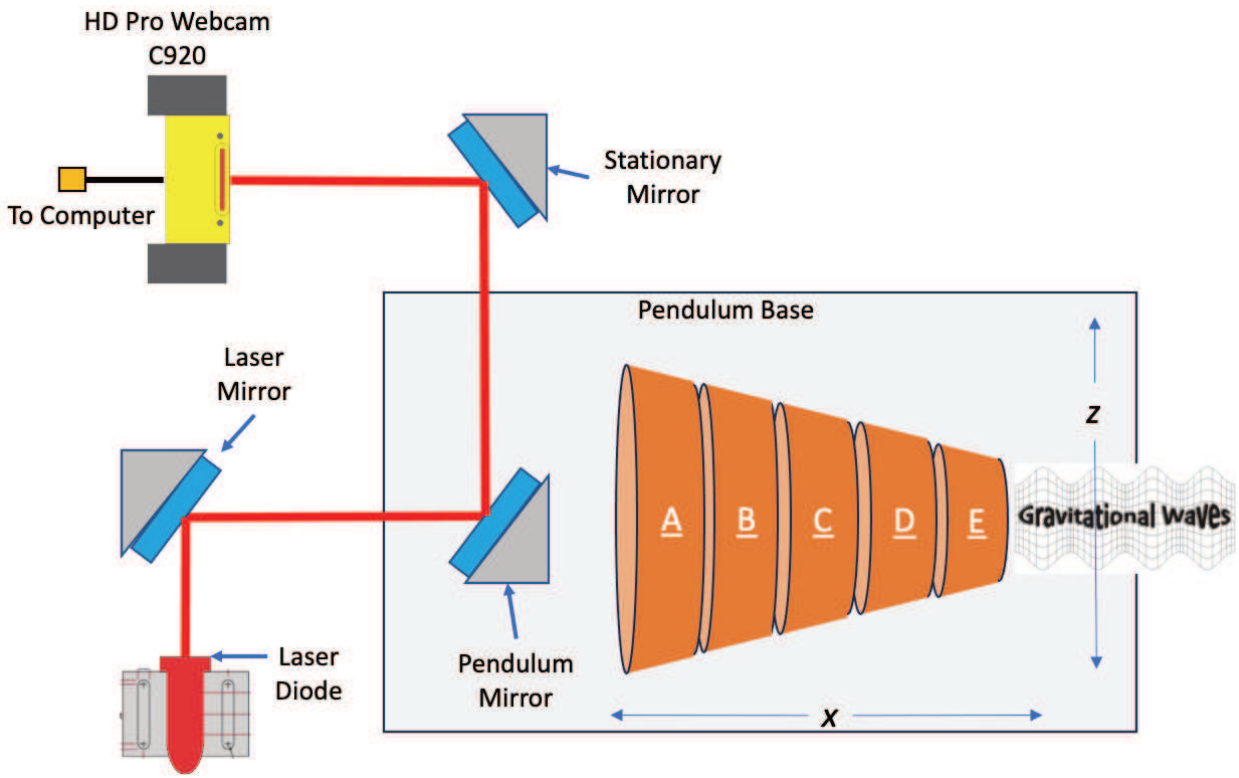

Figure 9
Top View of Test Configuration

Image Acquisition and Plotting

Figure 10 below shows a block diagram of the image acquisition configuration. The first is a webcam block that captures the laser beam image at thirty frames per second. The next block captures each 200x1920 pixel frame and sends it to a MATLAB function which senses the left and right beam movement by calculating the mean-of-a-histogram for each frame. A typical frame image is displayed in Figure 11 and a plot of the beam strength is shown in Figure 12. The Scope (in Figure 10) plots the movement of the beam in real time which is then stored for post processing.

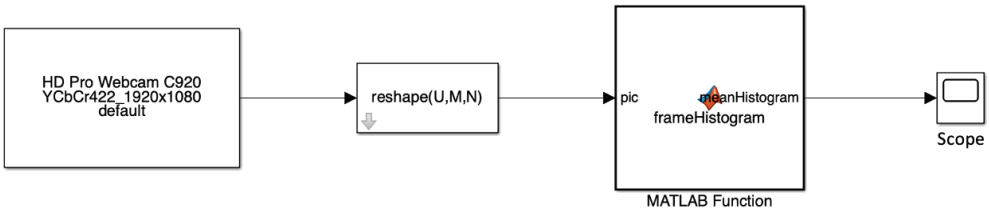

Figure 10 Webcam live image acquisition block diagram

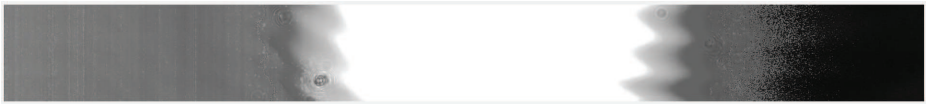

Figure 11 Camera image of laser beam: 200x1920 pixels

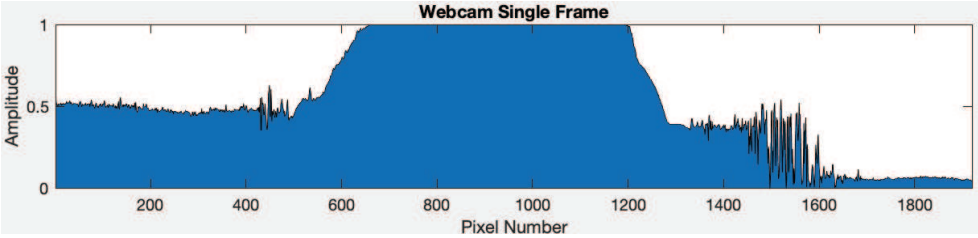

Figure 12 Plot of a single frame capture

The equation for calculating the mean of a histogram is:

$$\mu = \frac{1}{N}\sum_{i=0}^{M-1} iH_i$$

Where:
N is the number of points in the signal
M is the number of points in the histogram
H_i are the values of the sampled signal

```
% function to calculate mean of a histogram
for each frame capture

function meanHistogram = frameHistogram(pic)
  pixelWidth = 1920;
  mymean = 0;
  frameSum = 0;
  mm = transpose(mean(pic));
  for pixel = 1:pixelWidth
    mymean = mymean + pixel * mm(pixel);
    frameSum = frameSum + mm(pixel);
  end
  meanHistogram = mymean/frameSum;
```

Power Switch

Five switches were installed to control the power delivered to each RF amp (see Photo 9). During calibration, each RF amplifier was powered on individually while adjusting the phase and amplitude. Phase differences between CH 1 (reference) and CH 2 (antenna) were measured using an oscilloscope and a monopole antenna (see Figure 4).

Imitating Thrust Using Electromagnet

An electromagnet was included in the setup to determine what an actual (known) force on the pendulum testbed would look like. Figure 13 below plots the resulting pendulum displacement when power is applied to the electromagnet for a duration of 20 seconds.

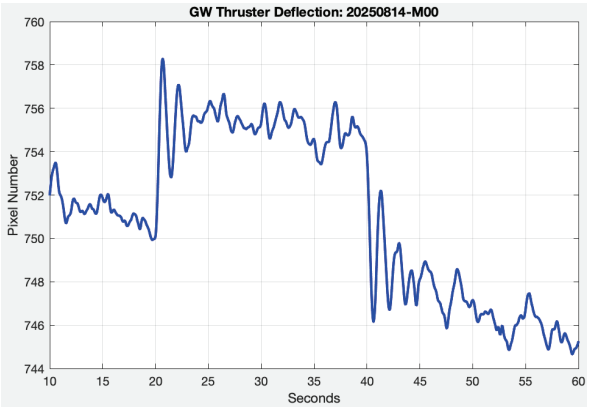

Figure 13
Measured displacement using test electromagnet.
Power applied between 20 and 40 second mark.

Test Results

Figure 14a below shows a polar plot of the set amplitude and phases of the five antenna elements. Figure 14b plots the measured signal amplitudes and phases of the five antenna elements during the test runs.

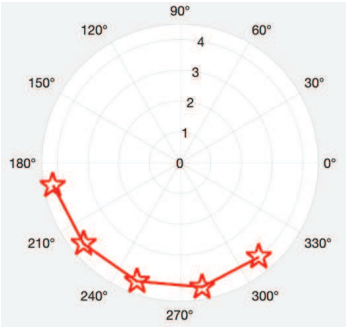

Figure 14a
Polar Plot
Amplitude and Phase

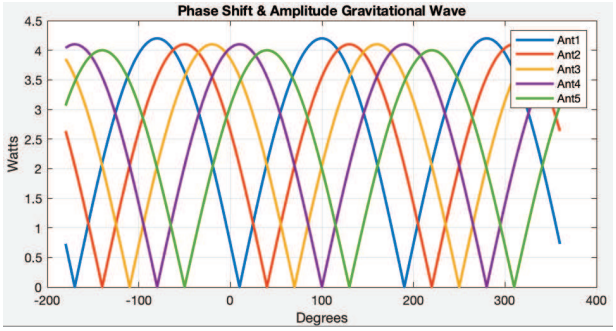

Figure 14b
Measured Amplitude and Phase Delay
2025-08-14
Phase = [-170;-140;-110;-80;-50]
Power = [4.2;4.1;4.1;4.1;4.0] Watts

A total capture time of 60 seconds was used for testing. No power was applied to the antenna array for the first 20 seconds; power was applied for 20 seconds and then shut off for the remaining 20 seconds. Figure 15a is a plot of the average of ten test runs, clearly showing that the antenna array moved to the left while power was applied to the device. Figure 15b is a plot of four typical test runs. The plot of Figure 15a shows that the total movement of the device was equal to 0.4 pixels of the line scan camera. (Each pixel is 2.86μm in width). Using the pendulum force equation (F = mgsinθ), the thrust generated by the GWT was calculated to be 45.27μN of force when a total of 20.5 Watts of RF power was applied to the antenna array.

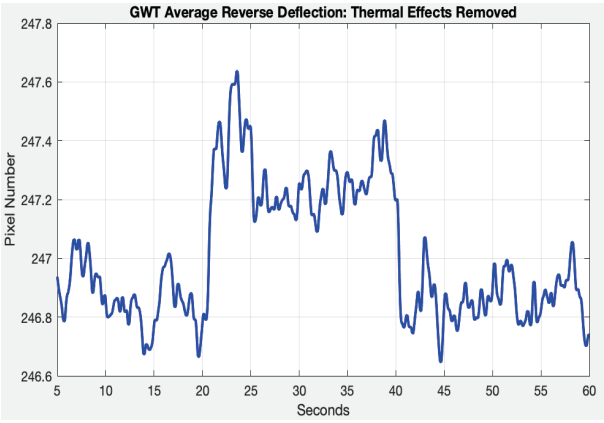

Figure 15a
Plot of average of 10 test runs
2025-08-14
Total deflection = 0.4 Pixels ←

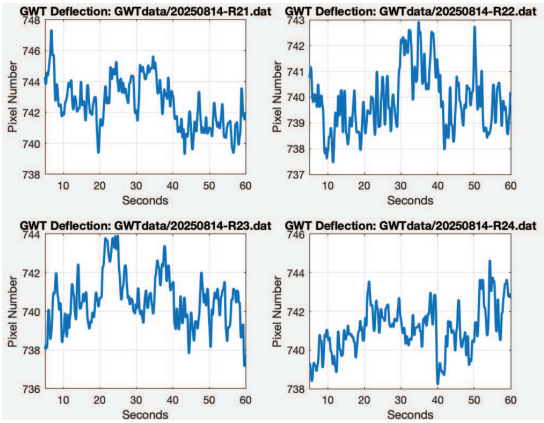

Figure 15b
Typical test runs
Reverse direction ←

Normally, the antenna array is rotated horizontally 180 degrees to produce thrust in the reverse direction. In this round of testing, however, the thrust reversed direction without the GWT device having been rotated. The phases were re-measured after the test runs. The measurements indicated that the phases of all five antenna elements shifted from their original settings during the tests runs. These results suggest that the adjustable phase shifters (Figure 4 and Photo 9) may not have sufficient long-term stability for predictable, consistent thrust.

Figure16a below is a plot of the average of the second series of ten test runs, clearly showing that the GWT moved in the opposite direction of the first series (see Figure 15a). Figure 16b is a plot of four typical test runs. The total average deflection measured was equal to 0.45 pixel widths when a total of 20.5 Watts of RF power was applied to the antenna array. This calculates to a force of 50.92μN.

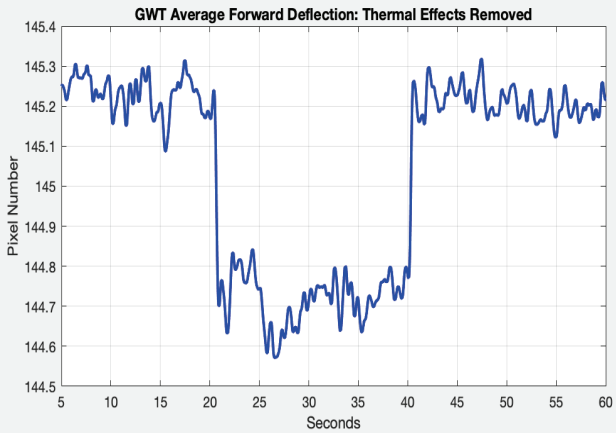

Figure 16a
Plot of average of 10 test runs
2025-08-14
Total deflection = 0.45 pixels →

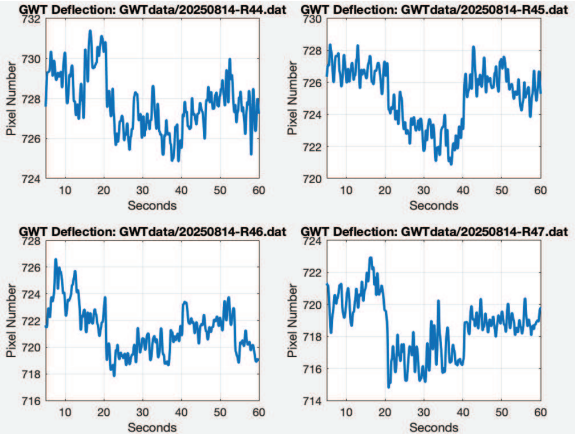

Figure 16b
Typical test runs
Forward direction →

Figures 17a and 17b illustrate the theoretical plots anticipated for both forward and reverse thrust scenarios.

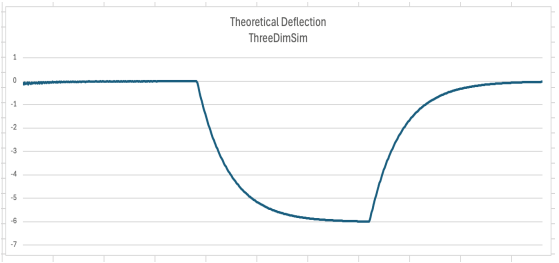

Figure 17a
Theoretical deflection
in forward direction →

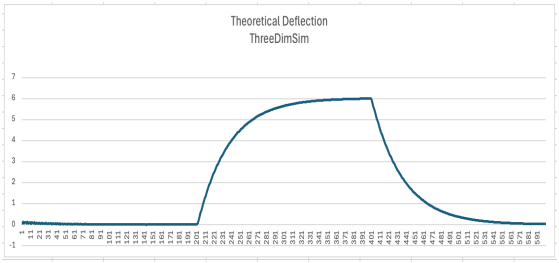

Figure 17b
Theoretical deflection
in reverse direction ←

Table 1 gives a summary of the results with data that includes pendulum force and thrust efficiency.

Test Date	Direction of Deflection	Deflection in Pixels	Deflection µm	Power Watts	Pendulum Force µN	Thrust Efficiency µN/Watt
2025-08-14	Left (reverse)	0.40	1.144	20.5	45.27	2.208
2025-08-14	Right (forward)	0.45	1.287	20.5	50.92	2.484

Table 1 Test Result Summary

Conclusion

According to the Foamy Ether Theory (FET), electromagnetic (EM) waves and gravitational waves (GWs) are regarded as distortions within the foamy ether. In this framework, EM wave distortions are transverse relative to their propagation direction, whereas GW distortions manifest as longitudinal compression waves, analogous to sound waves. This perspective indicates that EM waves can be manipulated to generate gravitational waves. Figures 2a–2f present simulation snapshots illustrating this process. The use of EM waves to produce GWs allows for the development of devices capable of continuous thrust without relying on propellants, as EM waves may be generated solely through electrical input. Consequently, such devices are particularly advantageous for space travel, given their capacity for indefinite operation provided an uninterrupted supply of electricity is available.

Discussion

Frequent adjustments to frequency, phases and power levels were necessary to generate an effective signal for the antenna array. The circuitry was prone to interference. Device components required adjustments whenever anything was modified. And the impedance matching circuit, attenuators and phase shifters required retesting and recalibrating each time the system was powered up. A high degree of confidence was established when a minimum of ten consecutive test runs yielded consistent results. The ten test runs were then averaged to reduce random noise, and plots were adjusted to counter thermal effects, thereby producing cleaner plots. Test results have confirmed that thrust is indeed produced. The unexpected reversal in thrust direction during testing indicates, however, that the stability of the adjustable (analogue) phase shifters and/or programmable attenuators is less than satisfactory. Computer controlled digital phase shifters and attenuators may offer some improvements in future testing processes.

Going Forward

The next phase involves obtaining additional testing from an independent second party. Additional validation will be provided by constructing a second device with a comparable design that generates thrust via gravitational waves. Testing the device within a vacuum

chamber is necessary to eliminate possible sources of thrust, such as heat dissipation, magnetic interference, or static electric forces.

References

[1] P. C. Hahn, "Foamy (A)ether Theory - A Framework for a Theory Of Everything," [Online]. Available: peterhahn.ca. [Accessed 11 2024].

[2] Quoro, "What is the ratio of electrostatic force and gravitational force of two electrons?," [Online]. Available: https://www.quora.com/. [Accessed 11 2024].

[3] P. M. Sutter, "In a Comprehensive new Test, the EmDrive Fails to Generate any Thrust," UNIVERSE TODAY, 2 4 2021. [Online]. Available: https://www.universetoday.com/150754/in-a-comprehensive-new-test-the-emdrive-fails-to-generate-any-thrust/.

[4] edy555, "About NanoVNA," [Online]. Available: https://nanovna.com. [Accessed 11 2024].

[5] EA6TY, "SimNEC for Interactive RF Circuit Analysis," [Online]. Available: https://www.ae6ty.com/smith_charts/. [Accessed 11 2024].

[6] Redwood Plastic and Rubber, "Redwood Plastic and Rubber," 01 01 2025. [Online]. Available: https://www.redwoodplastics.com.

[7] US National Science Foundation, "LIGO," [Online]. Available: https://www.ligo.caltech.edu. [Accessed 11 2024].

[8] European Gravitational Observatory, "Virgo," [Online]. Available: https://www.virgo-gw.eu. [Accessed 11 2024].

[9] KAGRA, "KAGRA Project," [Online]. Available: https://gwcenter.icrr.u-tokyo.ac.jp/en/. [Accessed 11 2024].

[10] P. C. Hahn, "Design for a Time Variance - Gravitational Wave Detector," 02 04 2020. [Online]. Available: https://vixra.org/abs/1506.0137.

[11] NASA, "James Webb Space Telescope," [Online]. Available: https://science.nasa.gov/mission/webb/. [Accessed 11 2024].

[12] NASA, "Hubble Space Telescope," [Online]. Available: https://science.nasa.gov/mission/hubble/. [Accessed 11 2024].

[13] M. Wade, "Calibration of the Advanced Laser Interferometer Gravitational-wave Observatory (LIGO) Detectors," 22 03 2016. [Online]. Available: https://physics.case.edu/events/calibration-of-the-advanced-laser-interferometer-gravitational-wave-observatory-ligo-detectors-madeline-wade/.

Photos

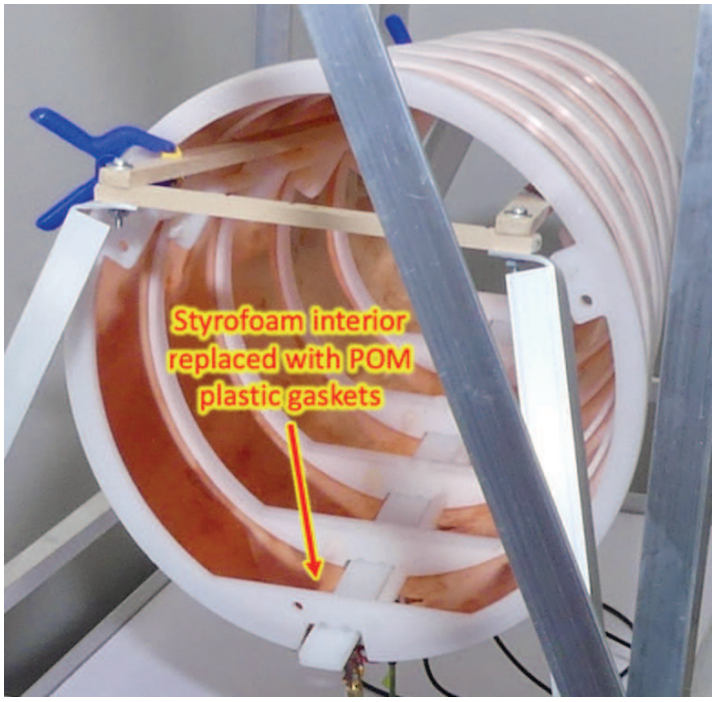

Photo 1
Antenna Array
Using POM Gaskets

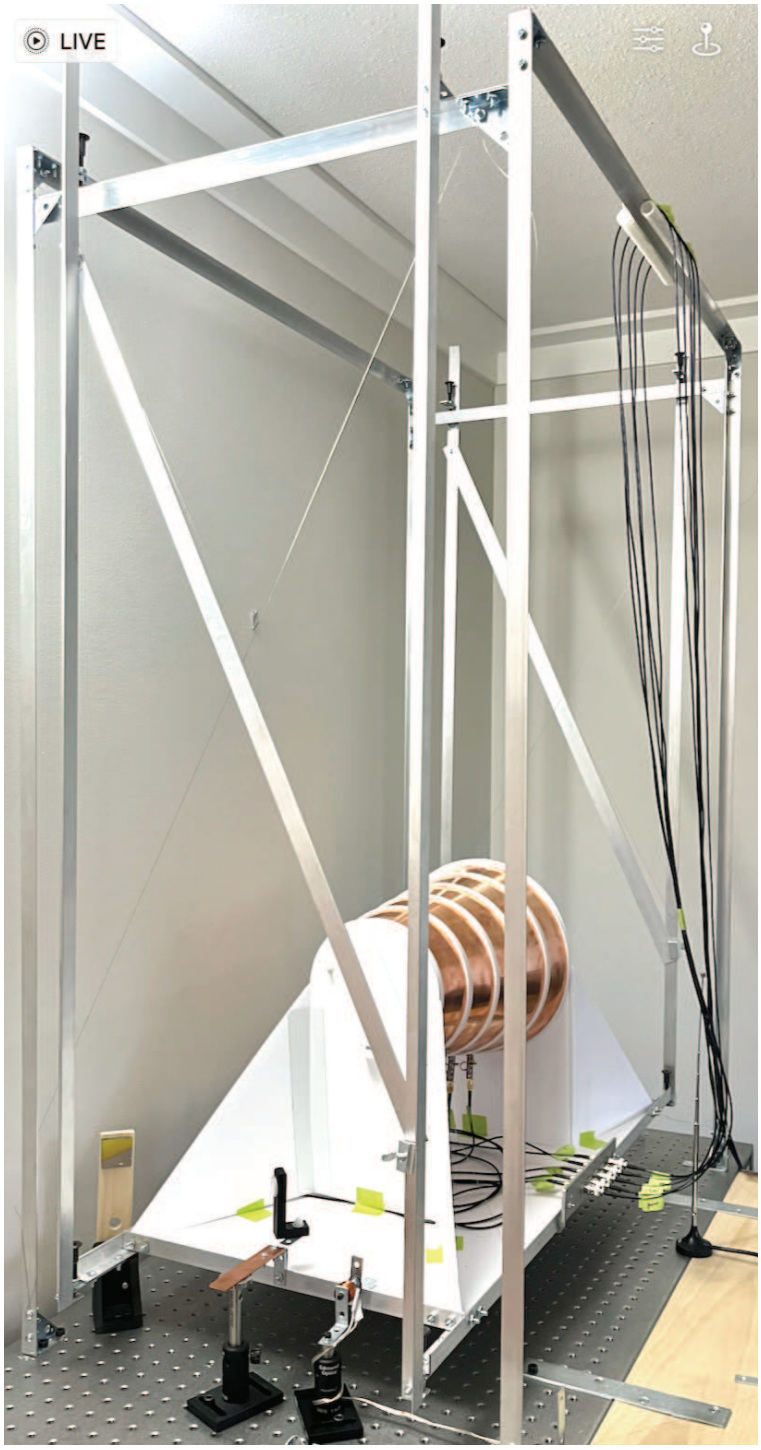

Photo 2
Antenna Array and
Pendulum Configuration
(Showing New Crossbeams and Cross wires)

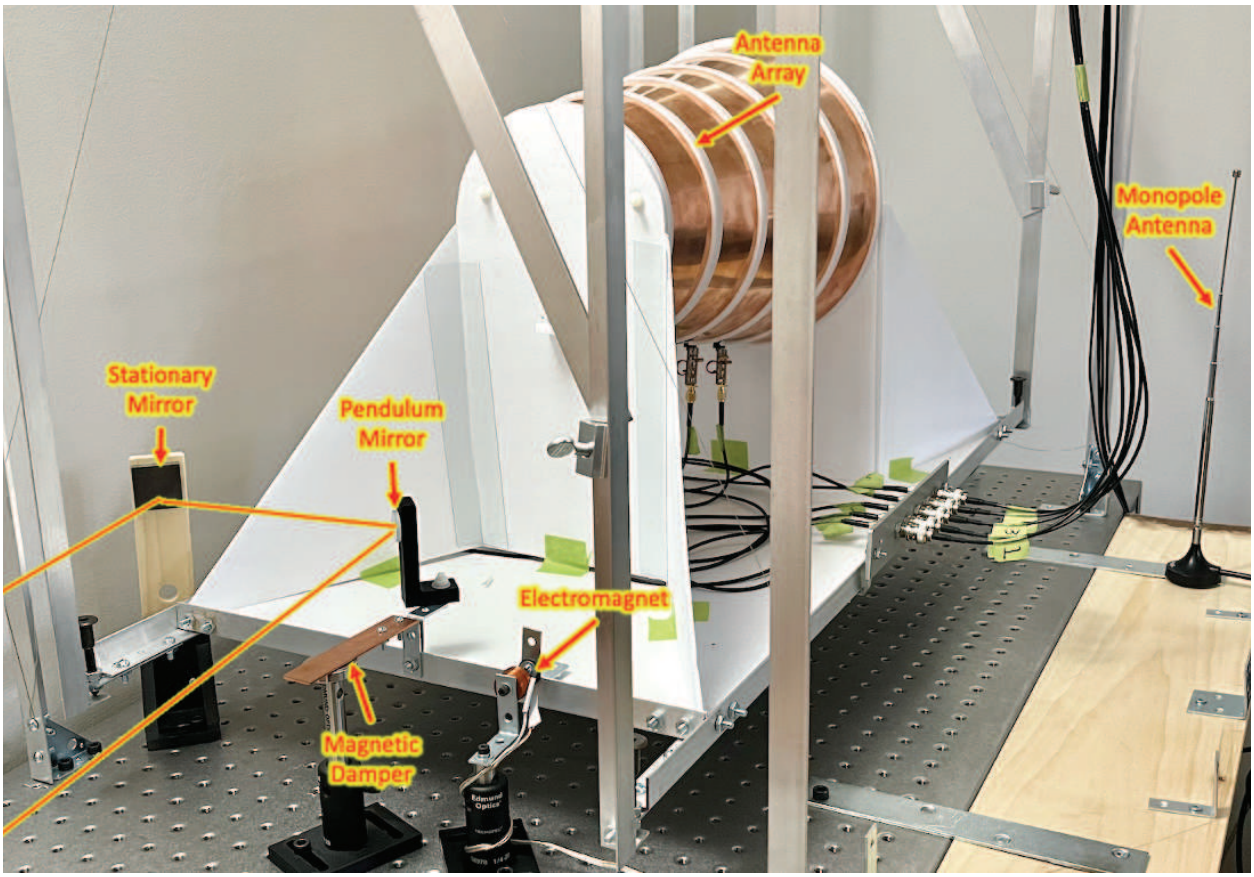

Photo 3
Pendulum Test Apparatus Components

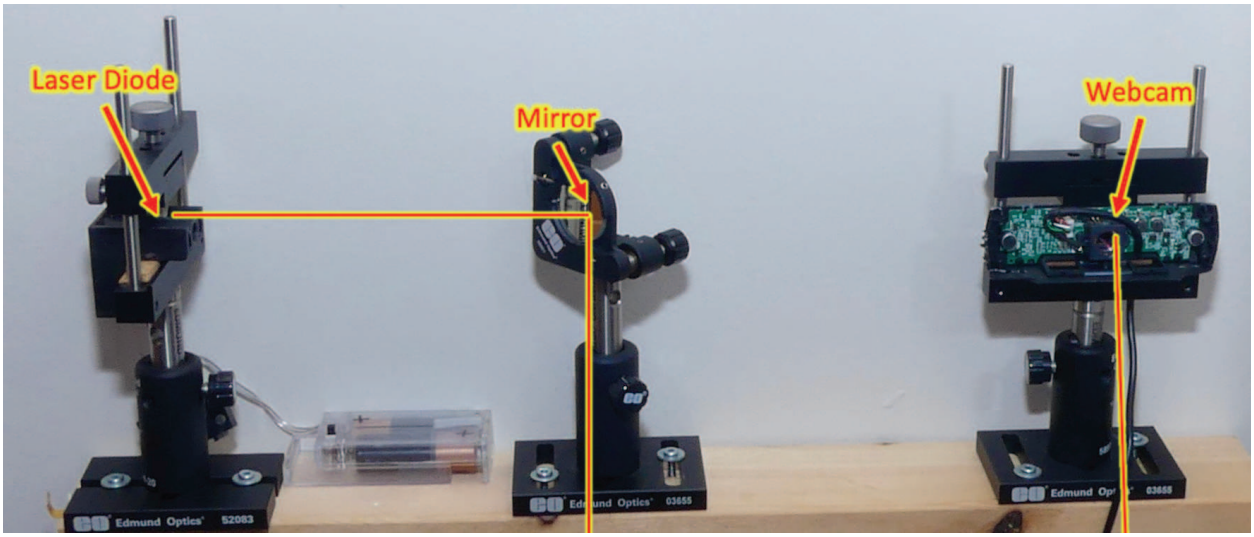

Photo 4
Laser, Webcam Test Apparatus Components

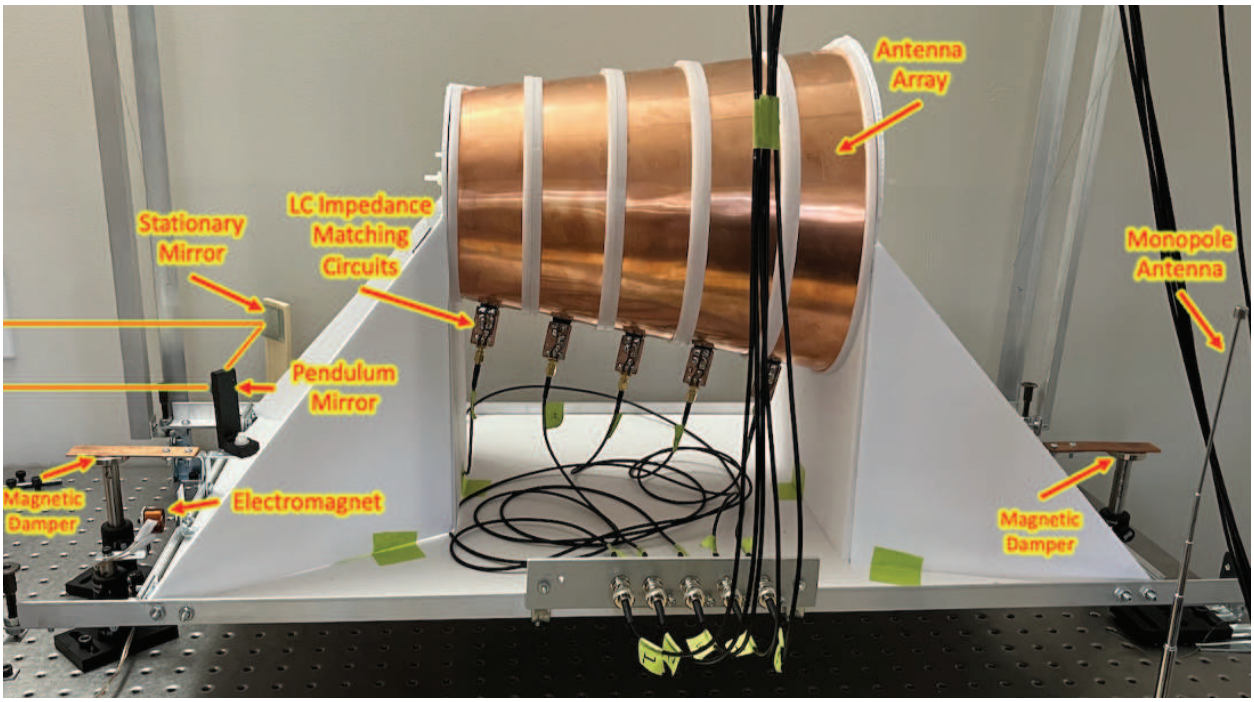

Photo 5
Side View Test Apparatus Components

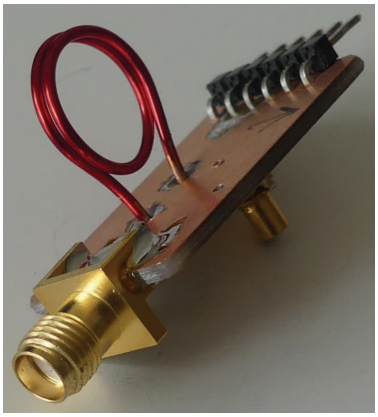

Photo 6
LC Circuit Board Showing Inductor:
Number of Turns: 2
Diameter: 11mm
Wire diameter: 1.024mm (18AWG)
Inductance: 71nH

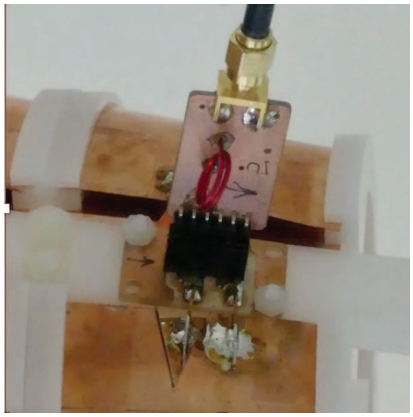

Photo 7
LC Circuit Board Connected to Antenna Array Element

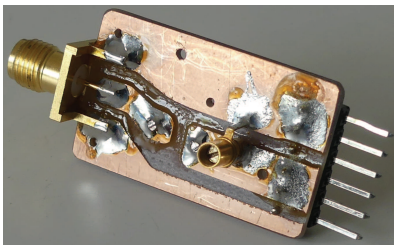

Photo 8
LC Circuit Board showing Adjustable Capacitor
https://www.knowlescapacitors.com
CAP TRIMMER 0.6-4.5PF 500V SMD **27273-3R5**

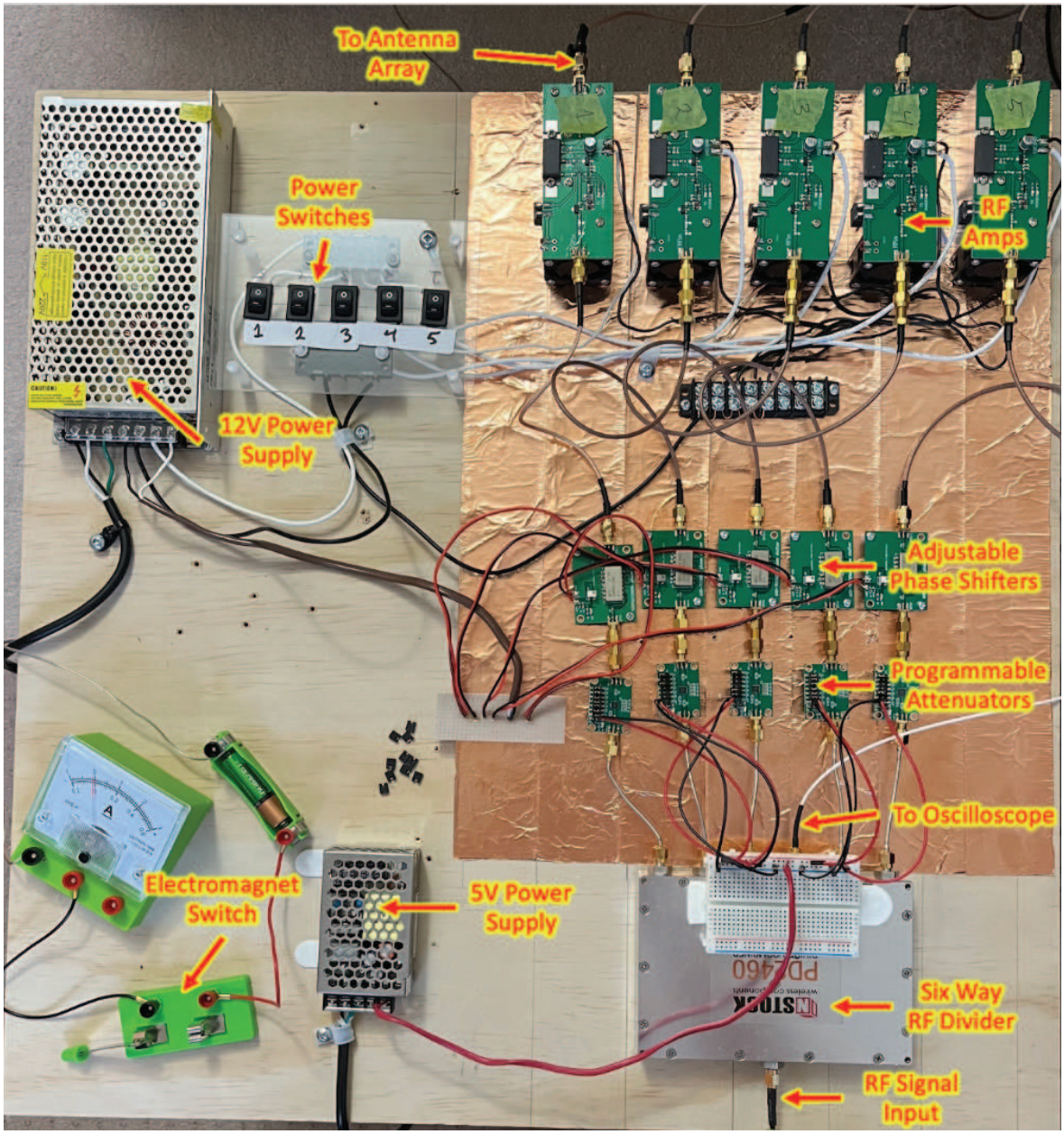

Photo 9 RF Feeder Circuitry